

Constitutive behavior and failure criteria for composites under static and dynamic loading

Isaac M. Daniel

Received: 29 August 2013 / Accepted: 19 October 2013 / Published online: 8 November 2013
© Springer Science+Business Media Dordrecht 2013

Abstract The technology of composite materials has experienced dramatic developments in the last four decades with continuously expanding applications. Further development depends to a great extent on the introduction of new material systems and a rapid evaluation of the resulting composites. To facilitate and accelerate this process, it is important to develop/establish comprehensive and effective methods and procedures of constitutive characterization and modeling and failure prediction of structural laminates based on the properties of the constituent materials and especially the basic building block of the composite, the single ply or lamina. The plethora of available composite failure theories coupled with a dearth of reliable experimental data provides no definitive answer as to the best general approach to failure prediction. A new failure theory recently developed at Northwestern University has been proven very successful in predicting failure of a composite lamina under multi-axial states of stress and varying strain rates in cases where the biggest discrepancies were observed in predictions by other theories.

Keywords Mechanical characterization of composites · Constitutive modeling · Failure criteria · Failure envelopes · Strain rate effects

1 Introduction

The technology of composite materials has experienced dramatic developments in the last four decades with ever expanding applications. Further development depends to a great extent on the design and introduction of new material systems and a rapid screening, evaluation, adoption and integration of these materials into the structural design. To facilitate and accelerate the process of introducing and evaluating new materials, it is important to develop/establish comprehensive and effective methods and procedures of constitutive characterization and modeling and failure prediction of structural laminates based on the properties of the constituent materials, e.g., fibers, nanoparticles, and polymers, and the basic building block of the composite structure, the single ply or lamina.

Composite materials in service are exposed to severe loading and environmental conditions which pose new challenges to the designer. In many structural applications composite materials are exposed to high energy, high velocity dynamic loadings producing multi-axial dynamic states of stress. Under these conditions composites exhibit nonlinear and rate-dependent behavior. Therefore, it is important to characterize experimentally the nonlinear dynamic behavior of composites under multi-axial states of stress and describe

I.M. Daniel (✉)
Robert R. McCormick School of Engineering and Applied
Science, Northwestern University, Evanston, IL 60208,
USA
e-mail: imdaniel@northwestern.edu

their behavior by appropriate constitutive models and failure theories.

Many test methods have been developed and discussed for characterization of composite materials at strain rates ranging from quasi-static to over $1,000 \text{ s}^{-1}$ [1–9]. In some cases explicit empirical relations were given for the rate dependence of mechanical properties [4, 6]. Studies have included biaxial stress states by testing off-axis composites [4, 6, 7, 9]. Modeling the nonlinear behavior observed in the tests above is a challenging task. Chen and Sun proposed a quadratic plastic potential function independent of dilatational deformation, by introducing elastic anisotropic parameters [10]. More recently, Yokozeki et al. extended Sun and Chen's model and proposed a two-parameter model that distinguishes between tension and compression of the plastic flow [11]. Several models have been proposed to account for strain rate effects. They include models proposed by Sun and associates [12, 13], Goldberg and Stouffer [14], Zhu et al. [15]. These models make use of several parameters which must be determined by fitting to experimental data.

In recent research described by the author and his associates, composite materials were characterized under quasi-static and dynamic multi-axial states of stress [16, 17]. A new nonlinear constitutive model was proposed to describe their rate-dependent behavior under states of stress including tensile and compressive loading [17]. The proposed potential function consists of a linear combination of deviatoric and dilatational deformation components. Experimental results were in very good agreement with predictions of the proposed constitutive model.

Failure of composite materials has been investigated extensively from the physical and phenomenological points of view, on microscopic and macroscopic scales. On the micromechanical scale, failure initiation and failure mechanisms vary widely with type of loading and are intimately related to the mechanical, physical and geometric properties of the constituent phases, i.e., matrix, reinforcement, interface/interphase and reinforcement architecture (e.g., fiber packing and lamination stacking sequence) [18–30]. Micromechanics can yield predictions of local failure at critical points. However, such predictions are only approximate as they do not relate easily to global failure of a lamina and failure progression to ultimate failure of a multi-directional laminate and composite structure.

On the macromechanical lamina scale, numerous failure theories have been proposed for analysis of composites and reviewed in the literature [31–42]. The plethora of theories is accompanied by a dearth of suitable and reliable experimental data, which makes the selection of one theory over another rather difficult. A “Worldwide Failure Exercise” was organized and conducted recently over a twelve-year period for the purpose of assessing the predictive capabilities of current (at the time) failure theories [34–38].

A recent development is a new failure theory developed at Northwestern University (NU-Daniel theory) which has been proven very successful in predicting failure of a composite lamina under multi-axial states of stress and varying strain rates [43, 44]. This theory addresses a class of problems where other theories differ the most from each other. The challenge now is to adapt and extend this new theory to the analysis of progressive failure of multi-directional structural laminates under multi-axial static and dynamic loadings and offer easily implemented engineering design tools.

2 Constitutive modeling of composite lamina

Two unidirectional material systems were investigated, AS4/3501-6 and IM7/8552 carbon/epoxy composites. The first one displays quasi-brittle behavior, has been studied more extensively and there is a large body of data available for it. The second system has a higher strength carbon fiber and displays a higher degree of nonlinearity and ductility. In addition, two textile composites were investigated, a carbon/epoxy fabric composite (AGP 370-SH/3501-6) and a woven glass/vinylester. Multi-axial experiments were performed by testing unidirectional carbon/epoxy specimens at various loading directions with respect to the principal fiber reinforcement. These experiments produced primarily stress states combining transverse normal and in-plane shear stresses.

Experiments were conducted at three strain rates. Quasi-static tests were conducted in a servohydraulic testing machine at a strain rate of 10^{-4} s^{-1} . Intermediate rate tests were also conducted in the servohydraulic machine at an average strain rate of 1 s^{-1} . High strain rate tests were conducted by means of a split Hopkinson pressure bar at strain rates ranging from 180 to 400 s^{-1} using prismatic off-axis specimens (Fig. 1). The Hopkinson bars were 12.7 mm in diameter and

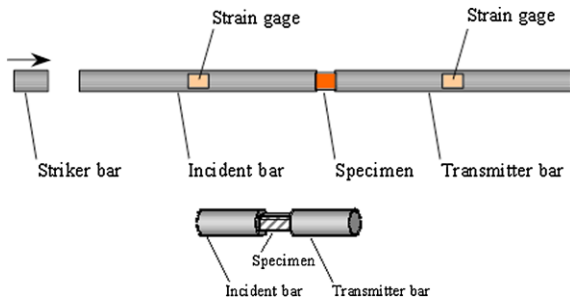


Fig. 1 High rate testing of composite specimens in Hopkinson bar

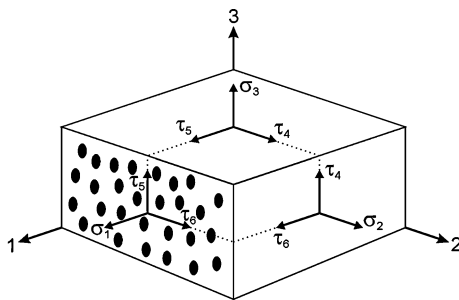


Fig. 2 Unidirectional composite element under load along the principal material axes

were made of high strength steel (Vascomax C-350). The specimens needed to be large enough to represent a characteristic volume of the material with a minimum aspect ratio of at least 2:1 to insure uniaxial stress. They also had to be short enough to allow for dynamic equilibration of stresses at the two ends of the specimen within a short time compared to the duration of the dynamic loading pulse. The composite specimens were prismatic with dimensions of 12.7 mm in length and 6.5 × 8.0 mm in cross section.

Composite materials, even those with quasi-brittle matrices, display nonlinear inelastic behavior. An element of a unidirectional composite under load along the principal material axes is shown in Fig. 2.

In the general nonlinear elastic plastic stress-strain response, the total strain increment corresponding to an increment in stress can be decomposed into an elastic and a plastic part as

$$d\varepsilon_i = d\varepsilon_i^e + d\varepsilon_i^p \tag{1}$$

The plastic strain increment is related to a potential (or loading) function through the associated flow rule and normality rule as follows

$$d\varepsilon_i^p = d\lambda \frac{\partial f}{\partial \sigma_i} \tag{2}$$

where $i = 1, 2, \dots, 6$, f is a plastic potential function and $d\lambda$ is a scalar function of proportionality.

A nonlinear constitutive model was proposed by the writer and his associates to describe the rate-dependent behavior under multi-axial states of stress including tensile and compressive loading [16, 17]. The proposed model describes the multi-axial stress-strain behavior measured at various strain rates and accounts for the sign of the normal stress (tension or compression). A general three-dimensional potential function, f , or effective stress, $\bar{\sigma}_e$, consisting of deviatoric and dilatational deformation components, was formulated for a transversely isotropic composite as

$$f = \{a_1[(\sigma_1 - \mu\sigma_2)^2 + (\sigma_1 - \mu\sigma_3)^2] + a_2(\sigma_2 - \sigma_3)^2 + a_4\tau_4^2 + a_6(\tau_5^2 + \tau_6^2)\}^{\frac{1}{2}} + [b_1\sigma_1 + b_2(\sigma_2 + \sigma_3)] = \bar{\sigma}_e \tag{3}$$

where a_1, a_2, a_4, a_6, b_1 and b_2 are plastic anisotropy parameters. The first bracketed term in Eq. (3) is related to shear deformation and the last (linear) bracketed term is related to dilatational deformation. The parameter μ is an elastic anisotropy parameter coupling normal stresses along the 1 and 2 and 1 and 3 directions and is related to the material stiffnesses.

For a two-dimensional state of stress, $\sigma_3 = \tau_4 = \tau_5 = 0$, the above expression is reduced to

$$f = \{a_1[(\sigma_1 - \mu\sigma_2)^2 + \sigma_1^2] + a_2\sigma_2^2 + a_6\tau_6^2\}^{\frac{1}{2}} + [b_1\sigma_1 + b_2\sigma_2] = \bar{\sigma}_e \tag{4}$$

The incremental stress-strain relation is

$$d\varepsilon_i = S_{ij}d\sigma_j + d\varepsilon_i^p \tag{5}$$

where S_{ij} is the material compliance tensor ($i, j = 1, 2, \dots, 6$).

The incremental plastic strain energy per unit volume is given in terms of the effective plastic strain as

$$dW_p = \sigma_i d\varepsilon_i^p = \bar{\sigma}_e d\bar{\varepsilon}_p \tag{6}$$

where $d\bar{\varepsilon}_p$ is the increment in the effective plastic strain. Replacing the plastic strain increment with the

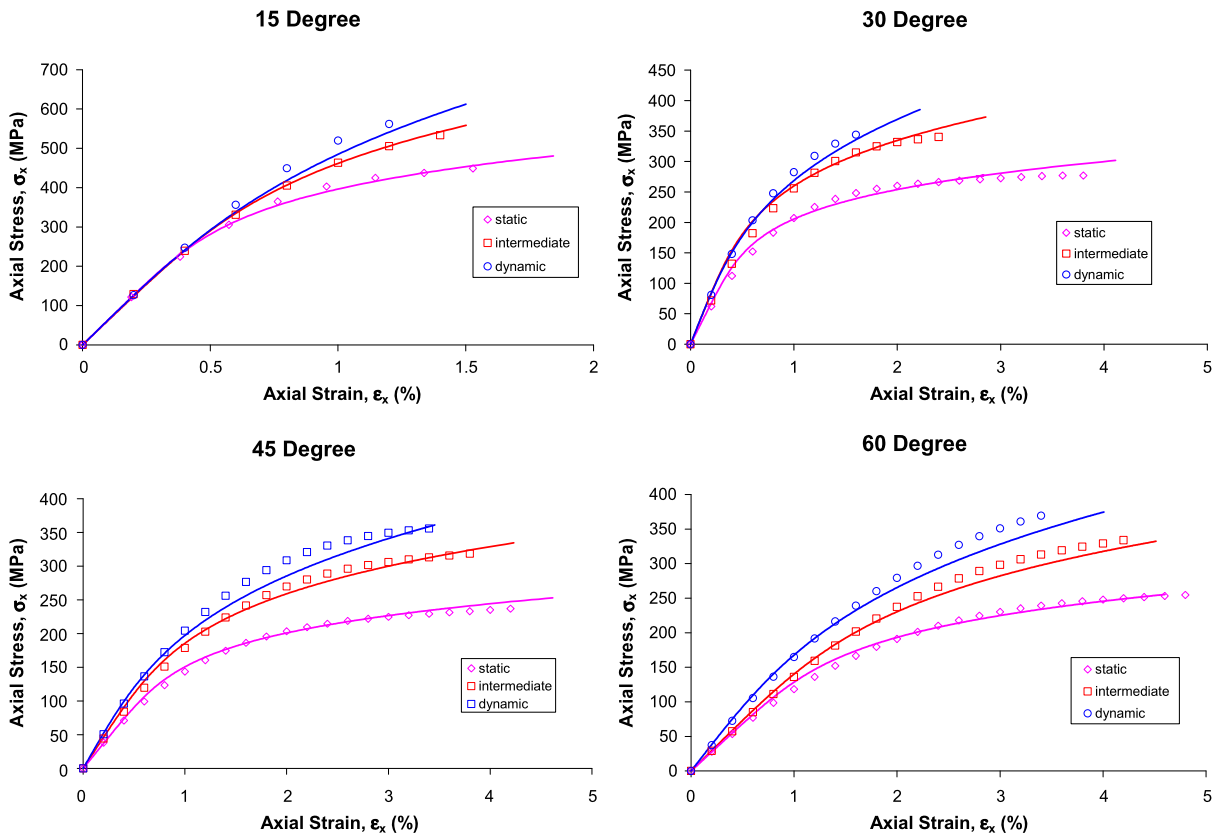


Fig. 3 Predicted and experimental stress–strain curves for carbon/epoxy composite loaded in compression at various orientations with the fiber direction at three strain rates [17]

gradient of the potential function by the flow rule (Eq. (2)),

$$\bar{\sigma}_e d\bar{\epsilon}_p = \sigma_i \frac{\partial f}{\partial \sigma_i} d\lambda = \bar{\sigma}_e d\lambda \tag{7}$$

Therefore, the scalar function of proportionality is given by

$$d\lambda = d\bar{\epsilon}_p \tag{8}$$

Assuming a power law relation between the effective plastic strain and effective stress as

$$\bar{\epsilon}_p = A\bar{\sigma}_e^n \tag{9}$$

with A and n functions of strain rate, we obtain the following expression for the scalar function

$$d\lambda = nA(\bar{\sigma}_e)^{n-1} d\bar{\sigma}_e \tag{10}$$

The incremental effective stress, from Eq. (4), is

$$d\bar{\sigma}_e = \frac{\partial f}{\partial \sigma_j} d\sigma_j \tag{11}$$

where $\sigma_j = \sigma_1, \sigma_2, \tau_6$.

Using Eqs. (5), (2), (8), (9), (10) and (11) we obtain the constitutive elasto/viscoplastic model for the total strain and stress increments as

$$d\epsilon_i = \left[S_{ij} - nA\bar{\sigma}_e^{n-1} \frac{\partial f}{\partial \sigma_i} \frac{\partial f}{\partial \sigma_j} \right] d\sigma_j \tag{12}$$

The yield criterion, assuming no plastic deformation in the fiber direction,

$$d\epsilon_1^p = d\lambda \frac{\partial f}{\partial \sigma_1} = 0 \tag{13}$$

yields $a_1 = b_1 = 0$ and the potential function, after normalizing by a_2 , is simplified as

$$f = \bar{\sigma}_e = \left[\sigma_2^2 + a_6 \tau_6^2 \right]^{\frac{1}{2}} + b_2 \sigma_2 \tag{14}$$

The model was validated experimentally for various states of biaxiality, tension and compression, and varying strain rates (Fig. 3). It is noted that the material behavior becomes more nonlinear for off-axis loadings at or near 45° with the fiber direction because of

the higher in-plane shear stress component. It is well known that unidirectional composites display highly nonlinear behavior in shear. The degree of nonlinearity decreases with increasing strain rate.

3 Failure theories

Most failure theories assume linear elastic behavior and are expressed in terms of macroscopic lamina stresses and strength parameters along the principal material axes (Fig. 2). These theories in general can be divided into three categories: (1) *Limit or non-interactive theories*, such as the maximum stress and maximum strain theories, (2) *Fully interactive theories* such as the Tsai-Hill and the Tsai-Wu criteria, and (3) *Partially interactive or failure mode based theories*, such as the Hashin-Rotem, Puck, and NU-Daniel theories. The popular fully interactive Tsai-Wu criterion is expressed as [31]

$$f_1\sigma_1 + f_2\sigma_2 + f_3\sigma_3 + f_{11}\sigma_1^2 + f_{22}\sigma_2^2 + f_{33}\sigma_3^2 + f_{44}\tau_4^2 + f_{55}\tau_5^2 + f_{66}\tau_6^2 + 2f_{12}\sigma_1\sigma_2 + 2f_{23}\sigma_2\sigma_3 + 2f_{31}\sigma_3\sigma_1 = 1 \tag{15}$$

where,

$$f_i = \frac{1}{F_{it}} - \frac{1}{F_{ic}}, \quad f_{ii} = \frac{1}{F_{it}F_{ic}} \quad (i = 1, 2, 3),$$

$$f_{44} = \frac{1}{F_4^2}, \quad f_{55} = \frac{1}{F_5^2}, \quad f_{66} = \frac{1}{F_6^2},$$

$$F_{it}, F_{ic}, F_4, F_5, F_6 = \text{tensile, compressive and shear strengths,}$$

$$f_{ij} \cong -\frac{1}{2}\sqrt{f_{ii}f_{jj}}$$

($ij = 12, 23, 31$, no summation implied)

The Hashin-Rotem criteria are based on the premise that failure on any plane is only a function of the stress components acting on that plane. Furthermore, separate fiber and interfiber failure modes are considered. Thus, for the composite element of Fig. 2, the criteria take the form

$$\frac{|\sigma_1|}{F_1} = 1$$

$$\left(\frac{\sigma_2}{F_2}\right)^2 + \left(\frac{\tau_4}{F_4}\right)^2 + \left(\frac{\tau_6}{F_6}\right)^2 = 1 \tag{16}$$

$$\left(\frac{\sigma_3}{F_3}\right)^2 + \left(\frac{\tau_4}{F_4}\right)^2 + \left(\frac{\tau_5}{F_5}\right)^2 = 1$$

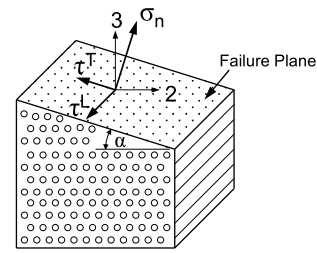


Fig. 4 Stress components acting on failure plane (Puck theory)

where,

$$F_i = \begin{cases} F_{it} & \text{when } \sigma_i > 0 \\ F_{ic} & \text{when } \sigma_i < 0 \end{cases} \quad (i = 1, 2, 3)$$

Predictions of the various theories, even for a simple unidirectional lamina, can differ a great deal from each other. Failure theories deviate the most from each other for states of stress involving transverse compression and interfiber shear, $\sigma_2 < 0$, τ_6 or $\sigma_3 < 0$, τ_5 .

The Puck and Shürmann theory is based on the concept of internal friction and a modified Coulomb-Mohr criterion [39]. Only stresses acting on the failure plane determine failure (Fig. 4). The internal friction under transverse compression increases the apparent shear strength. The orientation of the failure plane under compression is measured by separate testing and is considered as a material constant. The failure criterion is expressed in terms of the normal and shear stresses on the failure plane and two friction coefficients, η^T transverse and η^L parallel to the fibers, as

$$\left(\frac{\tau^T}{F_S^T - \eta^T \sigma_n}\right)^2 + \left(\frac{\tau^L}{F_S^L - \eta^L \sigma_n}\right)^2 = 1 \tag{17}$$

Sun et al. proposed an empirical modification of the Hashin-Rotem criterion for matrix compressive failure to account for the apparent increase in shear strength due to the transverse compressive stress ($\sigma_2 < 0$) [32]. The proposed criterion is:

$$\left(\frac{\sigma_2}{F_{2c}}\right)^2 + \left(\frac{\tau_6}{F_6 - \eta\sigma_2}\right)^2 = 1 \tag{18}$$

where η is an internal friction parameter.

4 Northwestern failure theory

The Northwestern (NU-Daniel) interfiber/interlaminar failure theory is based on micromechanical matrix failure mechanisms but is expressed in terms of easily

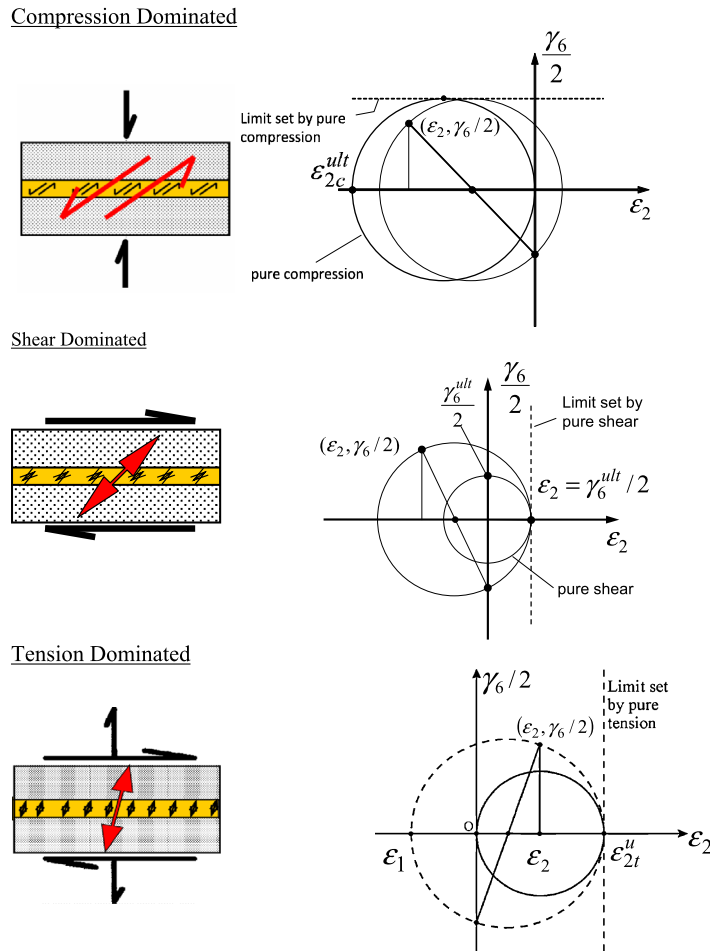


Fig. 5 Failure mechanisms in composite element and corresponding limiting strains in matrix layer

measured macromechanical properties. Three dominant failure mechanisms are identified in a composite element consisting of fibers and interfiber matrix, Fig. 5 [43].

In the compression dominated case, the composite element is loaded primarily in transverse compression with a non-dominant shear component. Failure is assumed to be governed by the maximum (critical) elastic shear strain in the interfiber matrix while the strain along the fiber is constrained to be zero. Relating this critical strain to the macroscopic stresses and compressive strength we obtain the following compression dominated failure criterion:

Compression dominated failure:

$$\left(\frac{\sigma_2}{F_{2c}}\right)^2 + \alpha^2 \left(\frac{\tau_6}{F_{2c}}\right)^2 = 1 \quad (\text{criterion NUa}) \quad (19)$$

In the shear dominated case, the composite element is loaded primarily in in-plane shear with a non-dominant compression component. Failure is assumed to be governed by the maximum (critical) elastic tensile strain in the interfiber matrix while constraining the strain component along the fibers. Relating this critical strain to the macroscopic stresses and shear strength of the composite we obtain the following shear dominated failure criterion:

Shear dominated failure:

$$\left(\frac{\tau_6}{F_6}\right)^2 + \frac{2}{\alpha} \frac{\sigma_2}{F_6} = 1 \quad (\text{criterion NUb}) \quad (20)$$

In the tension dominated case, the composite element is loaded primarily in tension with a non-dominant shear component. Failure is assumed to be governed by the maximum (critical) elastic tensile

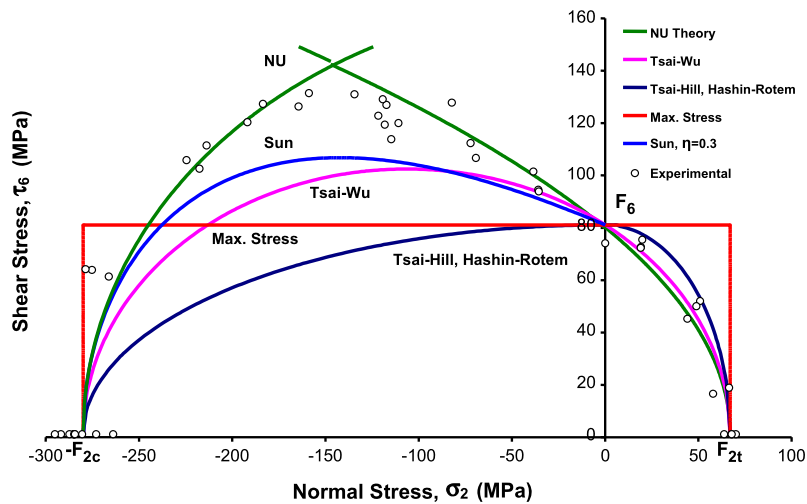


Fig. 6 Failure envelopes and experimental results for AS4/3501-6 unidirectional carbon/epoxy composite under in-plane shear and transverse normal loading [43]

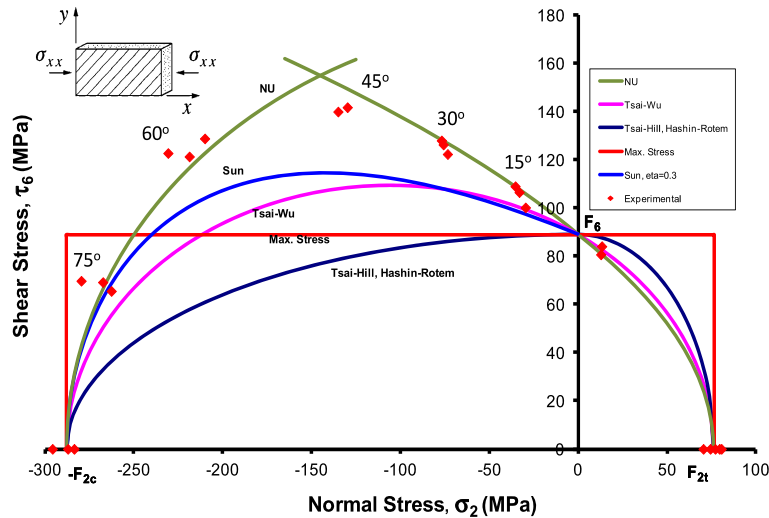


Fig. 7 Failure envelopes and experimental results for IM7/8552 unidirectional carbon/epoxy composite under in-plane shear and transverse normal loading [45]

strain in the interfiber matrix while constraining the strain component along the fibers. Relating this critical strain to the macroscopic stresses and transverse tensile strength of the composite we obtain the following tension dominated failure criterion:

Tension dominated failure:

$$\frac{\sigma_2}{F_{2t}} + \left(\frac{\alpha}{2}\right)^2 \left(\frac{\tau_6}{F_{2t}}\right)^2 = 1 \quad (\text{criterion NUc}) \quad (21)$$

where $\alpha = E_2/G_{12}$.

Figure 6 shows failure envelopes for a carbon/epoxy composite (AS4/3501-6) under matrix dominated states of stress (transverse compression, transverse tension and in-plane shear). It is shown how the NU-Daniel theory is in very good agreement with experimental results. Similar results were obtained for IM7/8552 carbon/epoxy (Fig. 7). The agreement with experimental results is very good, although the 8552 matrix is much more ductile than the 3501-6 matrix. This attests to the robustness of the NU-Daniel theory

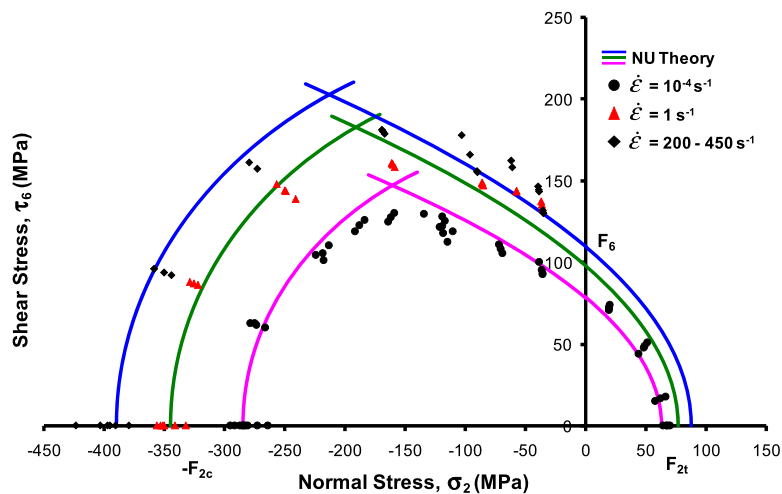


Fig. 8 Experimental results and failure envelopes predicted by the NU theory for AS4/3501-6 carbon/epoxy composite at three strain rates [44]

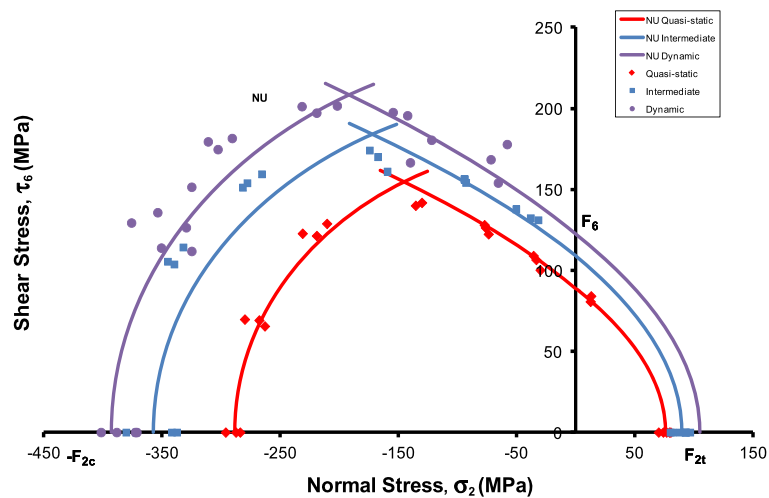


Fig. 9 Experimental results and failure envelopes predicted by the NU theory for IM7/8552 carbon/epoxy composite at three strain rates

which is governed by ultimate elastic strains irrespective of the nonlinear elastic and plastic behavior.

5 Strain rate effects

Stress-strain curves to failure of 90-deg and off-axis specimens of the two carbon/epoxy composites discussed before, were obtained at three different strain rates, quasi-static, intermediate and high. The basic strength parameters at different strain rates were used

in the failure criteria of Eqs. (19)–(21). Failure envelopes were plotted in Figs. 8 and 9 at three strain rates for the carbon/epoxy materials tested. The comparison between these failure envelopes predicted by the NU-Daniel theory and experimental results is very satisfactory.

The basic matrix dominated properties of the composite, including the initial transverse and in-plane shear moduli, E_2 and G_{12} , the transverse tensile and compressive strengths, F_{2t} and F_{2c} , and the in-plane shear strength, F_6 , were obtained from the tests at different strain rates. The strengths, normalized by their

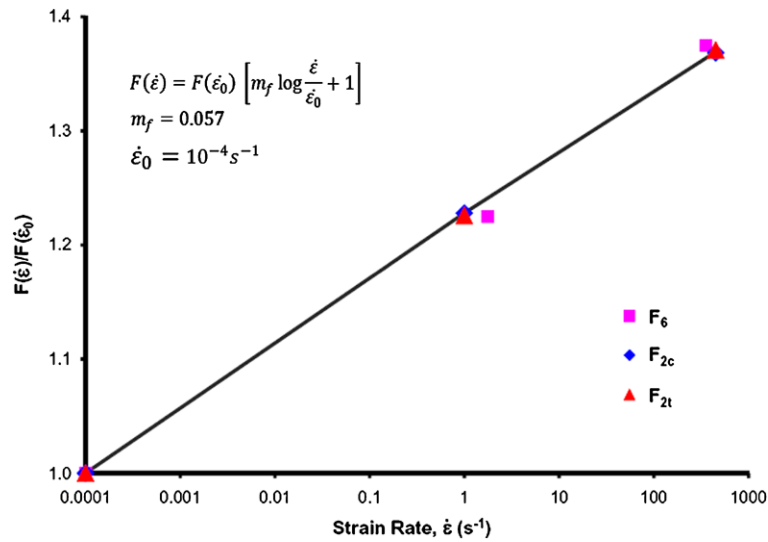


Fig. 10 Variation of transverse and shear strengths with strain rate

quasi-static values, were found to vary linearly with the logarithm of strain rate (Fig. 10). It appears that, for the range of strain rates considered, the variation with strain rate of the matrix dominated strengths can be described as

$$F(\dot{\epsilon}) = F(\dot{\epsilon}_0) \left(m \log_{10} \frac{\dot{\epsilon}}{\dot{\epsilon}_0} + 1 \right) \tag{22}$$

where,

$$F = \text{strength}(F_{2t}, F_{2c}, F_6),$$

$$m = 0.057,$$

$\dot{\epsilon}_0$ = reference strain rate

($\dot{\epsilon}_0 = 10^{-4} \text{ s}^{-1}$ for quasi-static loading).

In view of the results of Fig. 10 and Eq. (22), the failure criteria of Eqs. (19)–(21) are recast in a normalized form incorporating the strain rate effects as follows [44]:

Compression dominated failure:

$$\left(\frac{\sigma_2^*}{F_{2c}} \right)^2 + \alpha^2 \left(\frac{\tau_6^*}{F_{2c}} \right)^2 = 1 \quad (\text{criterion NUa}) \tag{23}$$

Shear dominated failure:

$$\left(\frac{\tau_6^*}{F_6} \right)^2 + \frac{2}{\alpha} \left(\frac{\sigma_2^*}{F_6} \right) = 1 \quad (\text{criterion NUb}) \tag{24}$$

Tension dominated Failure:

$$\frac{\sigma_2^*}{F_{2t}} + \frac{\alpha^2}{4} \left(\frac{\tau_6^*}{F_{2t}} \right)^2 = 1 \quad (\text{criterion NUc}) \tag{25}$$

where,

$$\sigma_i^* = \sigma_i \left(m \log \frac{\dot{\epsilon}}{\dot{\epsilon}_0} + 1 \right)^{-1}, \quad \sigma_i = \sigma_2, \tau_6 \tag{26}$$

and

$$\alpha = E_2/G_{12} \quad (\text{independent of strain rate})$$

Based on the above generalized criteria, the failure envelopes of Figs. 8 and 9 collapse into the normalized master envelopes shown in Figs. 11 and 12.

6 Multi-directional laminates

For a given loading condition, the first stage of failure in a multi-directional laminate is the so-called first-ply-failure (FPF), i.e., the loading at which the first ply or group of plies begins to fail [41]. Prediction and characterization of FPF is a challenging task and defines the capability of a given theory to predict ultimate failure. First-ply-failure is determined by conducting a stress analysis of the laminate under the given loading conditions, determining the state of stress in each individual layer, and assessing the strength of each layer by applying a selected failure criterion. This assumes that a layer or lamina within the laminate exhibits the same properties and behavior as an isolated unidirectional lamina. This is questionable, however, because the in-situ properties of an

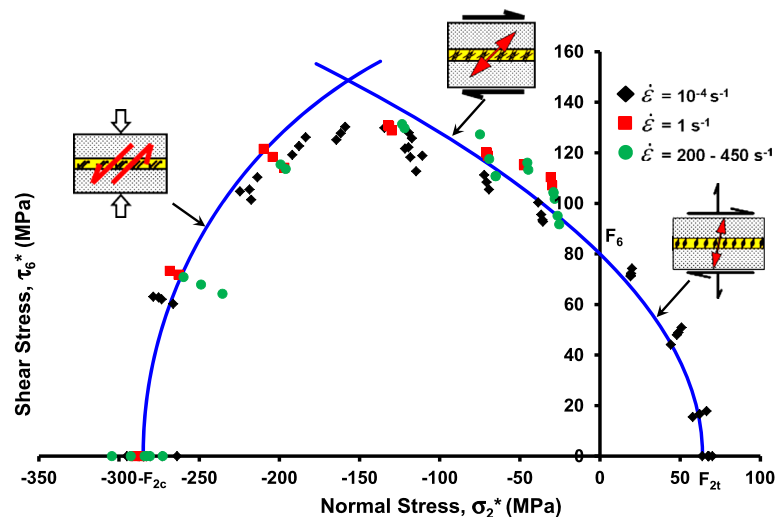


Fig. 11 Master failure envelope for AS4/3501-6 carbon/epoxy composite for strain rates in the range of 10^{-4} to 450 s^{-1} [44]

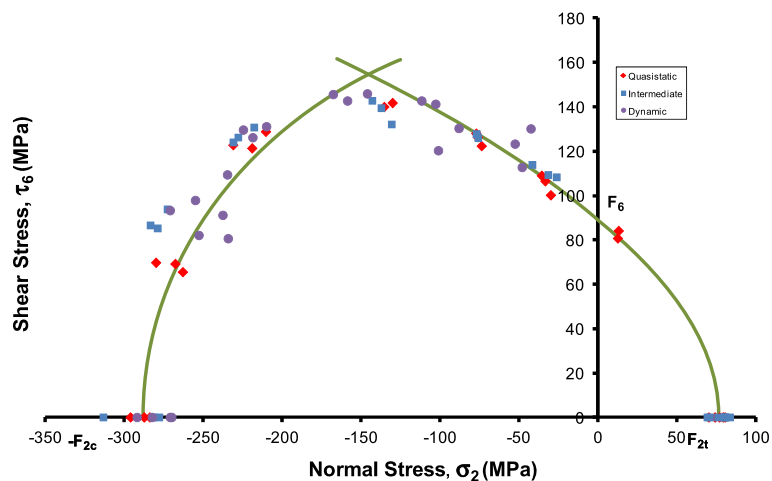


Fig. 12 Master failure envelope for IM7/8552 carbon/epoxy composite for strain rates in the range of 10^{-4} to 800 s^{-1} [45]

embedded layer may be different from those of an isolated layer. A layer within the laminate is constrained by adjacent plies and is under a state of fabrication residual stresses. Predictions of first-ply-failure can vary a great deal depending on the failure criterion used. Figure 13 shows first-ply-failure envelopes for crossply and quasi-isotropic carbon/epoxy laminates loaded under biaxial normal and shear stresses.

Lamina failure within a laminate takes the form of dispersed damage (microcracking) rather than a major localized flaw or crack. This microcracking progresses up to a limiting state, referred to as the characteristic damage state (CDS). The latter is a guide for the ply

discounting scheme in subsequent progressive failure analysis of the laminate. The onset of first-ply-failure, damage mode, and damage progression to the limiting damage state of the ply are very much dependent on the strain rate. The failure modes of the failed lamina or laminae are identified as matrix/interfiber or fiber failures. The stiffnesses of the damaged lamina must be discounted depending on the failure mode. The usual damage of matrix microcracking degrades primarily the in situ transverse and in-plane shear moduli of the ply.

Lamina stresses are recalculated and checked against the selected failure criteria. The load is then

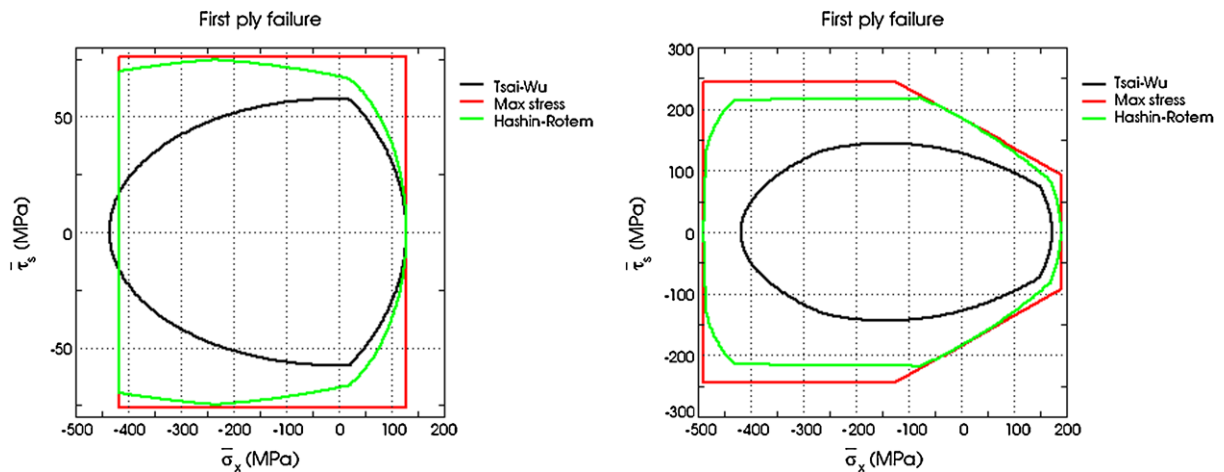


Fig. 13 Predicted first-ply-failure envelopes for carbon/epoxy laminates under biaxial normal and shear loading (a) crossply (b) quasi-isotropic

increased until the next ply, or group of plies, fails. Then, the above steps are repeated. The above process continues until the specified condition (or criterion) of ultimate laminate failure is met, e.g., maximum load, last ply failure (LPF) for matrix dominated failures, or first fiber failure (FFF) for fiber dominated failures.

In this study, carbon/epoxy (IM7/8552) angle-ply laminates of $[\pm\theta]_{14s}$ layup, were tested under uniaxial compression at two different strain rates (Fig. 14) [46]. This produces various levels of biaxial stress within the lamina for different angles, θ . In this case first-ply-failure occurs simultaneously in both layers and manifests itself as a gradual stiffness degradation corresponding to increasing matrix microcracking in the layers up to a limiting or saturation level (CDS). The stress at this characteristic damage state, σ_{cds} , is clearly defined in angle-ply laminates as the point of minimum or terminal modulus (Fig. 15). At this point the layer has reached maximum ply damage and, in an angle-ply laminate, it has reached the maximum stiffness reduction. For this reason, the characteristic damage state stress found experimentally for the various angle-ply laminates in compression was used to test the predictive capability of the NU-Daniel theory for laminates.

The characteristic damage state stress for the various laminates was obtained from the stress-strain curves of Fig. 14, by determining the laminate stress at which the terminal modulus is reached as shown in Fig. 15. Using the characteristic damage state stress, the residual stresses, and lamination theory, the lamina

stresses at the CDS level are determined and compared with the maximum ply damage envelope obtained by the NU-Daniel theory for the quasi-static and higher strain rates (Fig. 16). The original NU theory was developed for an isolated unidirectional lamina and is expressed in terms of the matrix dominated properties of the lamina, the stiffnesses, E_2 and G_{12} , and the strengths F_{2c} , F_{2t} , and F_6 . The shear strength used for the isolated lamina was obtained from a 10° off-axis tension test [41]. However, to account for the constraining effects within the laminate, an in-situ value of the shear strength, F_6 , was obtained from a $[\pm 45]_s$ compression test. This value of in-plane shear strength tends to be higher than the one obtained by the 10° off-axis test.

7 Summary and conclusions

An overview was given of recent and ongoing developments in characterization, constitutive modeling and failure prediction of composite materials. Composite materials were characterized under quasi-static and dynamic multi-axial states of stress. A new nonlinear constitutive model was proposed to describe their rate-dependent behavior under states of stress including tensile and compressive loading. The proposed potential function consists of a linear combination of deviatoric and dilatational deformation components. Experimental results were in very good agreement with predictions of the proposed constitutive model.

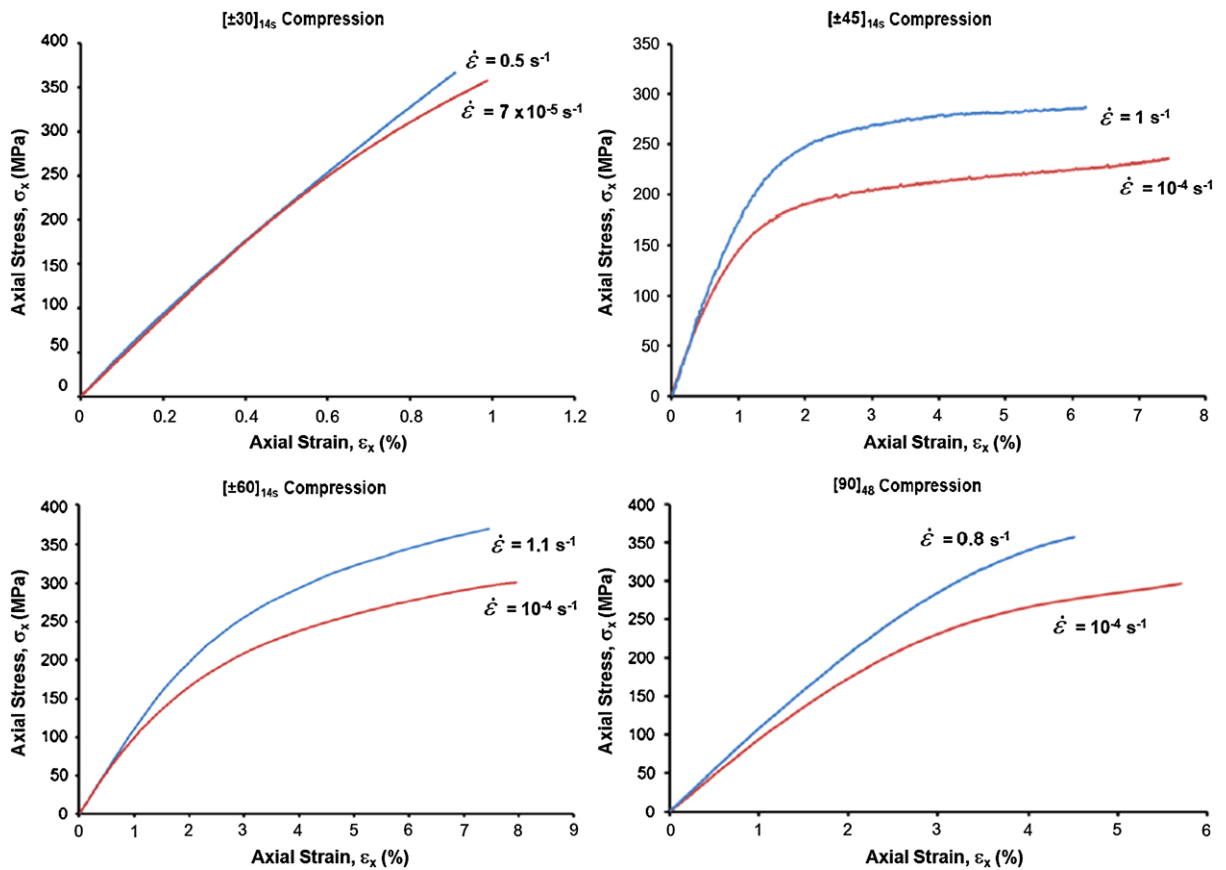


Fig. 14 Stress–strain curves under compression for 90-deg and angle-ply laminates at two strain rates (IM7/8552 carbon/epoxy) [46]

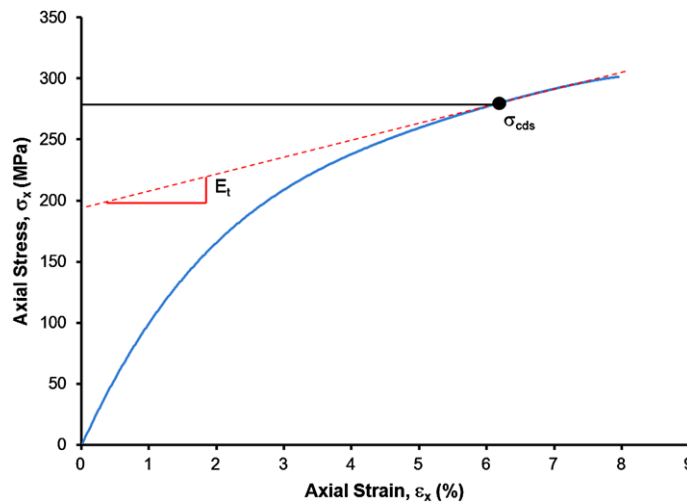


Fig. 15 Determination of characteristic damage state stress

A recent development is a new failure theory developed at Northwestern University (NU-Daniel the-

ory) which has been proven very successful in predicting failure of a composite lamina under multi-axial

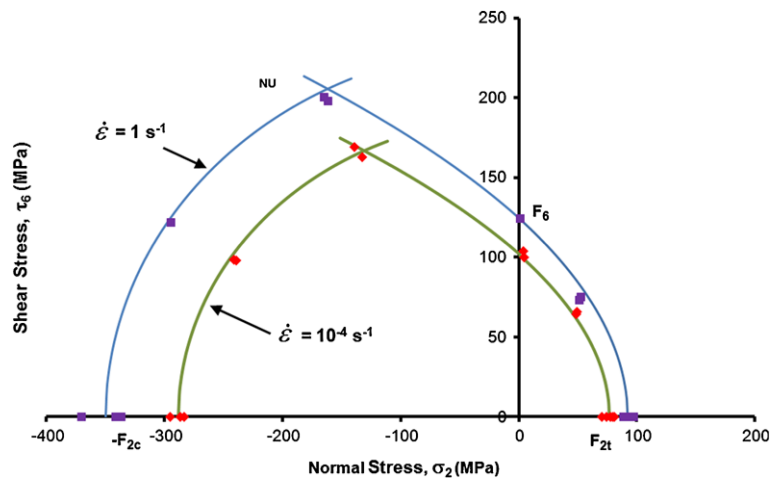


Fig. 16 NU theory prediction and experimental results for characteristic damage state of various angle-ply laminates at different strain rates (IM7/8552 carbon/epoxy) [46]

states of stress and varying strain rates. This theory addresses a class of problems where other theories differ the most from each other. One significant result of this theory is that it affords the designer easily implemented design and failure analysis tools. Furthermore, it may facilitate and accelerate the process of screening, evaluating and adopting new candidate materials in the industry.

The challenge now is to adapt and extend this theory to the analysis of progressive failure of multidirectional structural laminates under multi-axial static and dynamic loadings and offer easily implemented engineering design tools. Regarding progressive failure of multidirectional laminates, it is important to determine the maximum extent of damage that an individual layer can withstand. The NU theory does an excellent job in predicting damage saturation in layers of angle-ply laminates. This may also hold true for more complex laminates and it appears that using the characteristic damage state of the lamina is an excellent starting point for investigating progressive failure.

Acknowledgements This paper is being presented in this special issue of *Meccanica* published in honor of my esteemed colleague, Professor Emmanuel E. Gdoutos, on the occasion of his 65th birthday milestone.

The work described in this paper was sponsored by the Office of Naval Research (ONR). I am grateful to Dr. Y.D.S. Rajapakse of ONR for his encouragement and cooperation.

References

- Daniel IM, LaBedz R, Liber T (1981) New method for testing composites at very high strain rates. *Exp Mech* 21(2):71–77
- Sierakowski RL, Chaturvedi SK (1997) Dynamic loading and characterization of fiber reinforced composites. Wiley, New York
- Hsiao HM, Daniel IM (1998) Strain rate behavior of composite materials. *Composites, Part B, Eng* 29:521–533
- Hsiao HM, Daniel IM, Cordes RD (1999) Strain rate effects on the transverse compressive and shear behavior of unidirectional composites. *J Compos Mater* 33:1629–1642
- Li Z, Lambros J (1999) Determination of the dynamic response of brittle composites by the use of the split Hopkinson pressure bar. *Compos Sci Technol* 59:1097–1107
- Vinson JR, Woldesenbet E (2001) Fiber orientation effects on high strain rate properties of graphite/epoxy composites. *J Compos Mater* 35:509–521
- Ninan L, Tsai J, Sun CT (2001) Use of split Hopkinson pressure bar for testing off-axis composites. *Int J Impact Eng* 25:291–313
- Gilat A, Goldberg RK, Roberts GD (2002) Experimental study of strain-rate-dependent behavior of carbon/epoxy composite. *Compos Sci Technol* 62:1469–1476
- Koerber H, Xavier J, Camanho PP (2010) High strain rate characterization of unidirectional carbon-epoxy IM7-8552 in transverse compression and in-plane shear using digital image correlation. *Mech Mater* 42:1004–1019
- Chen JL, Sun CT (1993) A plastic potential function suitable for anisotropic fiber composites. *J Compos Mater* 27(14):1379–1390
- Yokozeki T, Ogihara S, Yoshida S, Ogasawara T (2007) Simple constitutive model for nonlinear response of fiber-reinforced composites with loading-directional dependence. *Compos Sci Technol* 67:111–118
- Weeks CA, Sun CT (1998) Modeling non-linear rate-dependent behavior in fiber-reinforced composites. *Compos Sci Technol* 58:603–611

13. Thirupukuzhi SV, Sun CT (2001) Models for the strain-rate-dependent behavior of polymer composites. *Compos Sci Technol* 61:1–12
14. Goldberg RK, Stouffer DC (2002) Strain rate dependent analysis of a polymer matrix composite utilizing a micromechanics approach. *J Compos Mater* 36:773–793
15. Zhu LF, Kim HS, Chattopadhyay A, Goldberg RK (2005) Improved transverse shear calculations for rate-dependent analyses of polymer matrix composites. *AIAA J* 43(4):895–905
16. Cho J, Fenner J, Werner B, Daniel IM (2010) A constitutive model for fiber reinforced polymer composites. *J Compos Mater* 44(26):3133–3150. doi:[10.1177/0021998309371547](https://doi.org/10.1177/0021998309371547)
17. Daniel IM, Cho J-M, Werner BT, Fenner JS (2011) Characterization and constitutive modeling of composite materials under static and dynamic loading. *AIAA J* 49(8):1658–1664
18. Hashin Z (1983) Analysis of composite materials—a survey. *J Appl Mech* 50:481–505
19. Whitney JM, McCullough RL (1990) Micromechanical materials modeling. Delaware composites design encyclopedia, vol 2. Technomic, Lancaster
20. Aboudi J (1991) Mechanics of composite materials—a unified micromechanical approach. Elsevier, Amsterdam
21. Gotsis PK, Chamis CC, Minnetyan L (1998) Prediction of composite laminate fracture: micromechanics and progressive failure. *Compos Sci Technol* 58(7):1137–1150
22. Gosse JH, Christensen S (2001) Strain invariant failure criteria for polymers in composite materials. In: 19th AIAA applied aerodynamics conference. doi:[10.2514/6.2001AIAA-1184](https://doi.org/10.2514/6.2001AIAA-1184)
23. Li R, Kelly D, Ness R (2003) Application of a first invariant strain criterion for matrix failure in composite materials. *J Compos Mater* 37:1977–2000
24. Tay TE, Tan SHN, Tan VBC, Gosse JH (2005) Damage progression by the element failure method (EFM) and strain invariant failure theory (SIFT). *Compos Sci Technol* 65:935–944
25. Li S (2000) General unit cells for micromechanical analyses of unidirectional composites. *Composites, Part A, Appl Sci Manuf* 32(6):815–826
26. Trias D, Costa J, Turon A, Hurtado JE (2006) Determination of the critical size of a statistical representative volume element (SRVE) for carbon reinforced polymers. *Acta Mater* 54(13):3471–3484
27. Matsuda T, Ohno N, Tanaka H, Shimizu T (2003) Effects of fiber distribution on elastic-viscoplastic behaviour of long fiber-reinforced laminates. *Int J Mech Sci* 45(10):1583–1598
28. Wongsto A, Li S (2005) Micromechanical finite element analysis of unidirectional fibre-reinforced composites with fibers distributed at random over the transverse cross-section. *Composites, Part A, Appl Sci Manuf* 36(9):1246–1266
29. Melro AR, Camanho PP, Pinho ST (2007) Generation of transversal material randomness in fibre-reinforced composites. In: Proc. of 16th international conference on composite materials, Kyoto, Japan
30. Hobbiebrunken T, Hojo M, Jin KK, Ha SK (2008) Influence of non-uniform fiber arrangement on microscopic stress and failure initiation in thermally and transversely loaded CF/epoxy laminated composites. *Compos Sci Technol* 68:3107–3113
31. Tsai SW, Wu EM (1971) A general theory of strength for anisotropic materials. *J Compos Mater* 5:58–80
32. Sun CT (2000) Strength analysis of unidirectional composites and laminates. In: Kelly A, Zweben C (eds) *Comprehensive composite materials*. Elsevier Science, Oxford, pp 641–666
33. Christensen RM (2001) A survey of and evaluation methodology for fiber composite material failure theories. In: Aref H, Phillips JW (eds) *Mechanics for a new millennium*. Kluwer Academic, Dordrecht
34. *Composites Science and Technology* (1998) *Compos Sci Technol* 58(7):999–1254
35. *Composites Science and Technology* (2002) *Compos Sci Technol* 62(12–13):1479–1797
36. *Composites Science and Technology* (2004) *Compos Sci Technol* 64(3–4):319–605
37. Hinton MJ, Soden PD, Kaddour AS (2004) Failure criteria in fibre-reinforced-polymer composites. Elsevier, Oxford
38. Hinton MJ, Kaddour AS, Soden PD (2002) A comparison of the predictive capabilities of current failure theories for composite laminates, judged against experimental evidence. *Compos Sci Technol* 62:1725–1798
39. Puck A, Shürmann H (2002) Failure analysis of FRP laminates by means of physically based phenomenological models. *Compos Sci Technol* 62:1633–1662
40. Davila CG, Camanho PP, Rose CA (2005) Failure criteria for FRP laminates. *J Compos Mater* 39(4):323–345
41. Daniel IM, Ishai O (2006) *Engineering mechanics of composite materials*, 2nd edn. Oxford University Press, New York
42. Daniel IM (2007) Failure of composite materials. *Strain* 43:1–9
43. Daniel IM, Luo J-J, Schubel PM, Werner BT (2009) Inter-fiber/interlaminar failure of composites under multi-axial states of stress. *Compos Sci Technol* 69:764–771
44. Daniel IM, Werner BT, Fenner JS (2011) Strain-rate-dependent failure criteria for composites. *Compos Sci Technol* 71(3):357–364
45. Schaefer JD, Werner BT, Daniel IM (2013) Strain rate effects on failure of a toughened matrix composite. In: Tandon GP et al (eds) *Experimental mechanics of composite, hybrid, and multifunctional materials*, vol 6. Springer, Berlin. doi:[10.1007/978-3-319-00873-8_15](https://doi.org/10.1007/978-3-319-00873-8_15)
46. Werner BT, Schaefer JD, Daniel IM (2013) Deformation and failure of angle-ply composite laminates. In: Tandon GP et al (eds) *Experimental mechanics of composite, hybrid, and multifunctional materials*, vol 6. Springer, Berlin. doi:[10.1007/978-3-319-00873-8_19](https://doi.org/10.1007/978-3-319-00873-8_19)